RSC Advances

PAPER

View Article Online
View Journal | View Issue

Cite this: *RSC Adv.*, 2025, **15**, 39194

Fundamental insights into the structural characteristic of dihydrogen-bonded complexes of $C_2H_{4-n}Cl_n\cdots MgH_2$ (n = 0, 1, 2, 3)

Lu Feng,[ac] Xianping Qiu,*[b] Yin-Si Ma,[a] Zhixiong Tian,[b] Kehai Chen,[b] Si Zhang,[b] Xiang Guo*[b] and Fu-Quan Bai *[a]

Received 24th May 2025
Accepted 14th October 2025

DOI: 10.1039/d5ra03654b

rsc.li/rsc-advances

At the MP2 computational method level, a systematic investigation has been conducted on the dihydrogen-bonded complexes formed by ethylene, its chlorine derivatives, and magnesium hydride. According to the optimized structures, the complexes under study are classified into three groups. The most stable among them are circular structures stabilized by CH⋯H and HMg⋯Cl bonds, with interaction energies ranging from 3.4 to 5.9 kcal mol^{-1}. The other group consists of linear structures, which are only stabilized by CH⋯H dihydrogen bonds and have relatively lower interaction energies between 0.5 and 2.0 kcal mol^{-1}. For all the investigated complexes, a slight elongation of the C–H bond is observed, accompanied by a red shift in its stretching frequency. As the number of chlorine atoms on the ethylene molecule increases, the geometries, frequencies, interaction energies of the complexes, and the electron density in the σ* antibonding orbital of C–H all show a gradual increase or decrease. Through atoms in molecules (AIM) and natural bond orbital (NBO) analyses, the nature of the electrostatic interaction in this type of dihydrogen bond has been revealed. By comparing the geometric data and AIM parameters, the effect of ring structures on dihydrogen bonding systems has been evaluated. Notably, the direction of net charge transfer in ring structure complexes is opposite to that previously observed in dihydrogen-bonded systems.

1. Introduction

Hydrogen bonds (HBs) have long been a focal point of scientific attention due to their pivotal roles across diverse fields. These include supramolecular chemistry, biochemistry, crystal engineering, energetic materials systems, and numerous emerging cross-disciplines intertwined with molecular science.[1–5] In these cases, an unusual type of hydrogen bonding, proton–hydride D–H⋯H–A interaction (where A is transition/alkali metal or boron and D is any electronegative atom/group) has attracted considerable attention.[6–8] Such interactions were named as dihydrogen bonds (DHBs) and have been investigated extensively since the mid-1990s by experimental[9–11] as well as theoretical methods.[12–15] Like conventional hydrogen bonds, dihydrogen bonds hold significant potential for applications in supramolecular synthesis and crystal engineering, while also playing a pivotal role in catalytic processes.[16] The unique ability of dihydrogen bonds to lose H_2 in the solid state, trading the weak H⋯H interactions for strong covalent bonds, promises new routes to the rational assembly of ordered, extended covalent materials.[17,18]

From X-ray and neutron diffraction experiments, it is known that D–H⋯H–A (A = boron, transition metal) systems have close H⋯H distances (1.75–1.90 Å), which is smaller than the sum of the van der Waals radii of the hydrogens (2.40 Å).[19] Their interaction enthalpies are significant (3–7 kcal mol^{-1}), falling within the range typically observed for conventional hydrogen bonds. Notably, Padilla-Martińez *et al.* have reported intramolecular C–H⋯H–B close contacts in aminoboron hydrides, which exhibit these characteristic interaction energies.[20] Their X-ray crystal structures show multiple H–H distances below 2.65 Å, which was considered the threshold intermolecular distance for H⋯H interactions in this study. The formation of dihydrogen-bonded complexes involving other main group hydrides—such as LiH, BeH_2, and the recently discovered XeH_2—has been theoretically investigated by numerous researchers.[12,21–23] To analyze complexes featuring exceptionally strong dihydrogen bonds, Grabowski *et al.* performed *ab initio* calculations at the MP2/aug-cc-pVDZ//MP2/aug-cc-pVTZ level of theory on the following systems: $H_2OH^+\cdots$HBeH, $H_2OH^+\cdots$HBeBeH, $H_2OH^+\cdots$HBeF, $HClOH^+\cdots$HBeH, $Cl_2OH^+\cdots$HBeH, and $Cl_2OH^+\cdots$HBeF.[24] According to the calculated results, the

[a]*Laboratory of Theoretical and Computational Chemistry, Institute of Theoretical Chemistry and College of Chemistry, Jilin University, Changchun 130023, People's Republic of China. E-mail: baifq@jlu.edu.cn*

[b]*National Key Laboratory of Aerospace Chemical Power, Xiangyang 441003, People's Republic of China. E-mail: guoxiang@casc42.cn; 77227820@qq.com*

[c]*Liaoning Petrochemical College, Department of Applied Chemistry, Jinzhou 121001, People's Republic of China*

shortest intermolecular H···H contact of 1.049 Å and the binding energy (corrected *via* BSSE) of 22.71 kcal mol^{-1} were predicted at the MP2/aug-cc-pVDZ level for the Cl_2OH^+···HBeH dimer. Thus, the criterion of H···H distances may be applied only as a first rough classification into the DHB systems. The review concerning the structures, energetics, and dynamics of the dihydrogen bonding has been published.[22] Based on all reports available, Custelcean and Jackson summarize that the interaction energies of DHB generally situated between 1 and 7 kcal mol^{-1}.

Regarding the C–H···H–A interaction, several theoretical studies on the DHB complexes formed by methane, acetylene and their derivatives with alkali metal hydride have been carried out,[25–28] and even C–H···H–C interactions were investigated.[29] For example, Lipkowski *et al.*[27] have studied the C–H···H dihydrogen-bonded complexes formed between CH_4 (and its fluoro and chloro derivatives) and LiH using *ab initio* methods, noting that the binding energy of these complexes increases with the number of fluoro or chloro substituents. Specially for the LiH···Y dimer, Cybulski *et al.* have classified the complexes into two groups,[30] based on the intermolecular distances and interaction energies: LiH···H_2, LiH···CH_4, and LiH···C_2H_6 as weak van der Waals complexes, LiH···C_2H_2 as dihydrogen-bonded strength complexes. It is worth noting that in the aforementioned C–H···H complexes, the carbon atom in the proton-donating C–H bond exhibits sp^3 or sp hybridization. In contrast, there have been few reports in the literature on investigations of dihydrogen bonding in ethylene and its derivatives, where the carbon atom involved in the proton-donating bond possesses sp^2 hybridization.[31–34] The $C_2H_{4-n}Cl_n$···NaH ($n = 0, 1, 2, 3$) complexes were analysed in our pervious study,[31] and it was found that an increase in the number of Cl-atom substituents leads to enhanced strength of the C(sp^2)–H···H dihydrogen bond. And for $C_2H_2Cl_2$(*trans*)···NaH and C_2HCl_3···NaH complexes, compared with the acyclic structure, which contains only one H···H contact, the formation of cyclic structures—characterized by H–Na···Cl and C–H···H interactions—results in a significant increase in the H···H bond length and influences the strength of the H···H interaction.

The purpose of the present study is to systematically investigate the properties of C(sp^2)–H···H interactions formed by another common alkali metal with AH_2 type. Thus as proton acceptor, we chosen the MgH_2, since it is a suitable hydride for experimental studies and has been proposed as a potential hydrogen storage material.[35] The studied complexes are divided into three groups (including linear structures, five- and six-membered cyclic structures) based on the optimized structures in present study. Unlike earlier $C_2H_{4-n}Cl_n$···NaH ($n = 0, 1, 2, 3$) system,[31] all the cyclic structure of $C_2H_{4-n}Cl_n$···MgH_2 ($n = 1, 2, 3$) complexes have an inverse direction of charge transfer (CT) which is contrary to the previous traditional DHB systems and decreased along with the augment of substituent Cl atoms. Aiming to this special CT character, the natural bond orbital (NBO) analysis is discussed. The 'atom in molecules' (AIM) methodology of Bader[36] is also applied to investigate the effect of cyclic structures on such DHB systems. We would like to emphasize that such dihydrogen bonding system have not been obtained from experiments or theoretical calculations elsewhere.

2. Theoretical methods

2.1 Methodology

All calculations here have been performed with the Gaussian 16 suite of programs.[37] To find a suitable level in order to discuss the structural parameters of C(sp^2)–H···H systems, we selected the C_2H_3Cl···MgH_2 complexes as test molecules. The methods considered include MP2, CCSD, QCISD and density functional theory with the B3LYP functional. The 6-311++G(d,p) basis set is of split-valence type including diffuse and polarization functions on hydrogen as well as heavy atoms. The optimized typical geometries data together with the interaction energies of selected complexes are reported in Table 1. The results in Table 1 suggest that the geometries optimized with B3LYP method are well consistent with the corresponding MP2 values. Two higher-order methods (CCSD(T) and QCISD) predicted much longer bond lengths and intermolecular contacts than those obtained with MP2 and B3LYP methods. Due to the lack of direct experimental data on present $C_2H_{4-n}Cl_n$···MgH_2 ($n = 0, 1, 2, 3$) system, the available experimental data relevant to geometry of MgH_2 molecule which is vibration–rotation emission spectrum have been employed for comparison with calculated results.[38] As can be seen in Table 1, all the theoretical methods overestimate the experimental Mg–H bond length in isolated MgH_2 molecule. However, the results from the MP2 and B3LYP calculations for MgH_2 monomer show much better agreement with experiment, in comparison with the results obtained by the CCSD(T) and QCISD methods. It means that MP2 and B3LYP methods give a more accurate account of geometry. Then, comparison of interaction energies obtained using MP2 and B3LYP methods in Table 1 reveals that the B3LYP method yields shallower energy minima for all selected complexes. In addition, the determination of the interaction energies using DFT methods has been proven to be insufficient in many cases to yield the accurate results which could interpret and guide the experimental investigations.[39,40] From a viewpoint of computational accuracy and efficiency, MP2/6-311++G(d,p) level appears to yield the most reliable geometries and interaction energies, which is consistent with the results reported in the literature.[25,41,42] To further verify the energetics, we performed CCSD(T)/CBS single-point calculations on the MP2-optimized geometries and found that this composite protocol yields interaction energies almost identical to those obtained at the bare MP2 level. Balancing cost,[43] consistency and accuracy, all geometrical investigations of monomers and complexes reported herein were conducted at the MP2/6-311++G(d,p) level.

2.2 Computation details

The interaction energies (ΔE_{int}) of all complexes were determined at the same theoretical level and corrected for basis set superposition error using the counterpoise method.[44] It is well established that the geometries of monomers in a complex deviate from their optimal isolated configurations.

Table 1 Optimized geometries and interaction energies (ΔE_{int}) for selected complexes, and Mg–H bond lengths of isolated monomers (r(H–Mg)$_{mono}$)[a]

Complex	Method	r(H···H)	r(C–H)	r(H–Mg)	r(H–Mg)$_{mono}$	r(Mg···Cl)	∠(C–H···H)	∠(H···H–Mg)	∠(H–Mg–H)	ΔE_{int}
$C_2H_3Cl\cdots MgH_2$(**L**)	MP2	2.3754	1.0847	1.7056	1.7044		174.1	175.0	179.9	1.01
	B3LYP	2.3824	1.0849	1.7053	1.7044		174.1	175.0	179.9	0.78
	CCSD(T)	2.4254	1.0859	1.7080	1.7074		174.1	175.0	180.0	0.93
	CCSD(CBS)	2.3754	1.0847	1.7056	1.7044		174.1	175.0	179.9	0.94
	QCISD	2.4264	1.0861	1.7082	1.7075		172.4	173.8	180.0	0.93
					1.7033 (ref. 37)					
$C_2H_3Cl\cdots MgH_2$(**S**)	MP2	2.3655	1.0839	1.7162		2.7467	143.5	105.3	163.0	4.96
	B3LYP	2.3448	1.0842	1.7151		2.8328	152.4	106.5	165.4	4.59
	CCSD(T)	2.3710	1.0851	1.7183		2.7583	146.3	105.3	162.8	4.71
	CCSD(CBS)	2.3655	1.0839	1.7162		2.7467	143.5	105.3	163.0	4.86
	QCISD	2.3325	1.0855	1.7184		2.7580	151.6	105.3	162.8	4.77
$C_2H_3Cl\cdots MgH_2$(**F**)	MP2	2.3661	1.0837	1.7218		2.7093	131.1	101.1	163.7	5.92
	B3LYP	2.3894	1.0823	1.7197		2.7986	133.0	102.2	165.4	5.33
	CCSD(T)	2.4156	1.0838	1.7234		2.7183	130.7	100.5	163.3	5.54
	CCSD(CBS)	2.3661	1.0837	1.7218		2.7093	131.1	101.1	163.7	5.65
	QCISD	2.4151	1.0840	1.7233		2.7178	130.7	100.5	163.4	5.53

[a] The 6-311++G(d,p) basis set is implied. Bond distance in Å, energies in kcal mol^{-1}, angle in degree.

Consequently, the deformation energy—defined as the energy required to deform monomers from their optimal equilibrium geometries to their configurations within the complex—has been subtracted. The Atoms in Molecules (AIM) methodology was applied to the *ab initio* results: critical points were identified, and an analysis of their characteristics was performed.[36] AIM calculations were conducted using the AIM2000 program.[45] To deepen into the nature of intermolecular interactions considered here, the natural bond orbital (NBO)[46] method was also applied. In the NBO analysis, the stabilization energy $E^{(2)}$ associated with delocalization $i \rightarrow j$ is estimated as:

$$E^{(2)} = \Delta E_{ij} = -n^{\sigma} F_{(i,j)}{}^2/(E_j - E_i)$$

In this expression, n^{σ} is the donor orbital occupancy, E_i and E_j are the donor and acceptor orbital energies, respectively, and $F_{(i,j)}$ is the Fock matrix element between i and j NBOs.

3. Results and discussion

3.1 Optimized structures and interaction energies

The $C_2H_{4-n}Cl_n\cdots MgH_2$ (n = 0, 1, 2, 3) complexes were fully optimized at the MP2/6-311++G(d,p) level of theory, with no imaginary frequencies detected for their respective monomers. $C_2H_2Cl_2$(*trans*), $C_2H_2Cl_2$(*cis*), and $C_2H_2Cl_2$(dic) correspond to *trans*-1,2-dichloroethylene, *cis*-1,2-dichloroethylene, and 1,1-dichloroethylene, respectively, which act as proton donors in dihydrogen-bonded (DHB) models. It is worth noting that for each of the $C_2H_3Cl\cdots MgH_2$, $C_2H_2Cl_2$(*trans*)$\cdots MgH_2$ and $C_2HCl_3\cdots MgH_2$ complexes, three structures corresponding to energetic local minima were obtained, whereas only two stable structures were identified for $C_2H_2Cl_2$(*cis*)$\cdots MgH_2$ on the potential energy surface. These structures are presented in Fig. 1. Complexes featuring only a C–H···H interaction are labelled as **L** structures, where the C, H, H, and Mg atoms adopt a collinear arrangement. For the remaining complexes, the coexistence of C–H···H and H–Mg···Cl interactions results in the formation of six-membered (**S**) or five-membered (**F**) cyclic structures. In the **S** and **F** structures, the C(sp^2)–H···H angles (129.7°–157.7°) are larger than the Mg–H···H angles (101.1°–107.8°), which is consistent with previous findings in dihydrogen-bonded (DHB) systems.[27] The formation of H–Mg···Cl interaction also results in obvious deformation of the H–Mg–H fragment from its linear form (see Fig. 1). Therefore, the deformation energy between the complex and the isolated monomer is taken into consideration of the calculation for the interaction energy (ΔE_{int}).

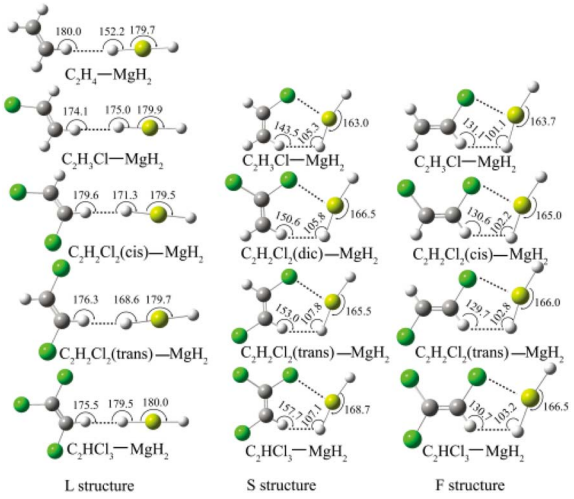

Fig. 1 Optimized structures for the $C_2H_{4-n}Cl_n\cdots MgH_2$ (n = 0, 1, 2, 3) complexes.

Table 2 Calculated results of C–H···H–Mg dihydrogen bonds at the MP2 level including H···H and Mg···Cl distances, variations of the C–H and H–Mg bond length (Δr) and vibrational frequencies ($\Delta\nu$), additionally C–H bond lengths of isolated monomers ($r(\mathrm{C–H})_{\mathrm{mono}}$) and interaction energies (ΔE_{int}) for DHB complexes[a]

Complex	r(H···H)	Δr(C–H)	$r(\mathrm{C–H})_{\mathrm{mono}}$	$\Delta\nu$(C–H)	Δr(H–Mg)	$\Delta\nu$(H–Mg)	r(Mg···Cl)	ΔE_{int}
L structure								
$C_2H_4\cdots MgH_2$	2.4978	0.0002	1.0854	−3	0.0008	2		0.53
$C_2H_3Cl\cdots MgH_2$	2.3754	0.0006	1.0841	−43	0.0011	6		1.01
$C_2H_2Cl_2(cis)\cdots MgH_2$	2.1425	0.0010	1.0831	−83	0.0017	10		1.77
$C_2H_2Cl_2(trans)\cdots MgH_2$	2.1386	0.0013	1.0829	−17	0.0005	12		1.69
$C_2HCl_3\cdots MgH_2$	2.0802	0.0020	1.0820	−30	0.0010	14		1.91
S structure								
$C_2H_3Cl\cdots MgH_2$	2.3655	0.0001	1.0838	−5	0.0117	−32	2.747	4.96
$C_2H_2Cl_2(dic)\cdots MgH_2$	2.2873	0.0013	1.0825	−10	0.0100	−24	2.801	3.66
$C_2H_2Cl_2(trans)\cdots MgH_2$	2.1867	0.0019	1.0829	−27	0.0125	−24	2.777	4.44
$C_2HCl_3\cdots MgH_2$	2.1449	0.0029	1.0820	−46	0.0111	−18	2.830	3.41
F structure								
$C_2H_3Cl\cdots MgH_2$	2.3661	0.0002	1.0836	2	0.0173	−31	2.709	5.92
$C_2H_2Cl_2(cis)\cdots MgH_2$	2.3225	0.0007	1.0831	−3	0.0172	−26	2.732	5.29
$C_2H_2Cl_2(trans)\cdots MgH_2$	2.3565	0.0008	1.0829	−7	0.0153	−20	2.746	4.75
$C_2HCl_3\cdots MgH_2$	2.2991	0.0014	1.0820	−17	0.0157	−22	2.757	4.54

[a] Bond distance in Å, energies in kcal mol^{-1}, frequencies in cm^{-1}.

The results displayed in Table 2 show that the H···H distances of all complexes, (except $C_2H_4\cdots MgH_2$ complex) lie in the range of 2.08 and 2.37 Å, smaller than the sum of the van der Waals H-radius (2.40 Å). And for a given structure (**L**, **F** or **S**), the H···H distances decrease as the number of chloro substituent increase. For the same proton donor, it can be observed that the length of the H···H contact in the **S** and **F** structures is longer than that in the **L** structure. Taking the $C_2HCl_3\cdots MgH_2$ complex as an example, the H···H distances for the **L**, **S**, and **F** structures are 2.080, 2.145, and 2.299 Å, respectively.

The bond length variations (Δr) and stretching frequency shifts ($\Delta\nu$) of the C–H and H–Mg bonds are summarized in Table 2. Similar to classical hydrogen bonds, the proton-donating C–H bonds in all complexes are elongated, and their stretching frequencies exhibit a red shift due to the formation of dihydrogen bonds—with the exception of the $C_2H_3Cl\cdots MgH_2$(**F**) complex, where the C–H bond is elongated but the frequency change is negligible. According to Grabowski *et al.*'s report, the elongation of donating bonds is greater for smaller H···H distances.[47,48] We can also observe this tendency for a given structures in $C_2H_{4-n}Cl_n\cdots MgH_2$ (n = 0, 1, 2, 3) complexes. Taking **S** structure as an example, the H···H distances for $C_2H_3Cl\cdots MgH_2$, $C_2H_2Cl_2(dic)\cdots MgH_2$, $C_2H_2Cl_2(trans)\cdots MgH_2$ and $C_2HCl_3\cdots MgH_2$ are 2.366, 2.287, 2.187 and 2.145 Å, and corresponding elongation values of Δr(C–H) are 0.0001, 0.0013, 0.0019 and 0.0029 Å, respectively. It is also worth to notice that for the same complex, the Δr(C–H) values are ordered as, **F** < **L** < **S**. After the analyses of the reported dihydrogen-bond properties, it is revealed that such bonds in the heterocyclic compounds are generally longer and weaker. For example, the H···H distance in the pyrrole···HLi complex (2.98 Å) already exceeds the sum of the van-der-Waals radii of two hydrogen atoms (2.40 Å), clearly moving beyond the weak-interaction regime.[34] This is mainly ascribed to the inherent stability of the conjugated framework and the preservation of aromaticity, which diminish the charge transfer capability of the surrounding H···H contacts. In contrast, the $Br_3CH\cdots HNa$ complex exhibits the shortest binding distance and the largest interaction energy. Overall, C(sp^3)–H···H interactions are stronger than those involving C(sp^2)–H···H, and the latter are weaker but leave space for the coexistence of other weak interactions.[49,50]

The elongation of the H–Mg proton accepting bond is observed in all the complexes, and this elongation is greater in **S** and **F** structures since HMg···Cl connection exists in these systems. For **L** structure, we can observe an increase of the H–Mg stretching frequency (blue-shift), while for **S** and **F** structures all results denoted distinct red shift. Additionally, for most complexes within **S** and **F** structures, the bond length variations (Δr) and stretch frequency shifts ($\Delta\nu$) of the H–Mg bond are larger than the corresponding value of C–H bond. These data suggest that the Mg–H proton-accepting bond is more sensitive than C–H proton-donating bond in **S** and **F** structures. Based on all the geometric parameters, it can be concluded that one dihydrogen bond is formed in $C_2H_{4-n}Cl_n\cdots MgH_2$ (n = 1, 2, 3) complexes.

The energetic parameters of the dihydrogen-bonded (DHB) systems are also summarized in Table 2. For **L** structures, the interaction energy (ΔE_{int}) values directly correspond to the strength of the dihydrogen bond, as each complex contains only one H···H contact. For **L** structures, with decreasing H···H contact distance, the interaction energies of $C_2H_4\cdots MgH_2$, $C_2H_3Cl\cdots MgH_2$, $C_2H_2Cl_2(cis)\cdots MgH_2$, $C_2H_2Cl_2(trans)\cdots MgH_2$, and $C_2HCl_3\cdots MgH_2$ are 0.53, 1.00, 1.77, 1.69, and 1.91 kcal mol^{-1}, respectively. This result indicates that for **L** structures, complexes with shorter H···H distances exhibit

higher stability, which is consistent with previous findings in DHB systems.[27] It is also indicated that the interaction energies of the complexes in **L** structure are smaller than those in **S** and **F** structures with HMg···Cl interaction. It is worth mentioning that increasing number of Cl-atom substituents lead to the decrease of the interaction energies in **S** and **F** structures. Additionally, this correlation has not been found in previous studied $C_2H_{4-n}Cl_n\cdots NaH$ (n = 0, 1, 2, 3) system.[31]

3.2 AIM analysis

In recent years, the AIM methodology has been applied to investigate dihydrogen-bonded systems.[27,40,47,51] In the Atoms in Molecules (AIM) theory, electron density (ρ) is used to characterize bond strength: the greater the ρ value, the stronger the bond. The Laplacian ($\nabla^2\rho$) describes the nature of the bond, where a negative Laplacian indicates a covalent bond, whereas a positive Laplacian signifies non-bonding or closed-shell interactions (such as ionic interactions or hydrogen-bonded species) between two atoms.[35] Popelier *et al.* proposed a set of criteria for the existence of hydrogen bond,[52] and Lipkowski *et al.* pointed out that the three criteria are the most fundamental and often applied:[27] for the identification of a bond critical point (BCP),[35] the electron density (ρ) and its Laplacian ($\nabla^2\rho$) should fall within the ranges of 0.002–0.035 a.u. and 0.02–0.15 a.u., respectively. Therefore, for the complexes analyzed herein, both the electron densities at the critical points and their Laplacians were considered, as these topological parameters can characterize the type of interaction. All results are summarized in Table 3.

All electron density values at the H···H bond critical points (BCPs) satisfy the criterion proposed by Popelier for hydrogen-bond interactions.[52] However, the situation differs for Laplacian values $\nabla^2\rho$: for the $C_2H_4\cdots MgH_2$ and $C_2H_3Cl\cdots MgH_2$(**L**) complexes, the Laplacians of electron density at the H···H BCPs fall below the lower limit, indicating that these interactions should be classified as van der Waals forces. For the remaining complexes, the Laplacian values are approximately 0.02–0.03 a.u., close to the lower threshold. Thus, based on the topological parameters of these complexes, classifying the interactions as hydrogen bonds remains equivocal. Furthermore, for a given structure type, a clear trend in the strength of H···H bonds within the $C_2H_{4-n}Cl_n\cdots MgH_2$ (n = 0, 1, 2, 3) series is observed from the ρ and $\nabla^2\rho$ values at the H···H BCPs, specifically: $C_2H_4\cdots MgH_2$ < $C_2H_3Cl\cdots MgH_2$ < $C_2H_2Cl_2$(*cis*, *trans* and dic)··· MgH_2 < $C_2HCl_3\cdots MgH_2$. This confirms that chlorine substitution enhances the H···H interaction. In most complexes, the electron density at C–H BCPs is higher, while that at H–Mg BCPs is lower, compared to the corresponding monomers. Additionally, the positive $\nabla^2\rho$ values at all H···H BCPs indicate the electrostatic character of the C(sp^2)–H···H interactions.

The values of $\rho_{H\cdots H}$ in $C_2H_2Cl_2$(*trans*)···MgH_2(**S**) and C_2H_2-Cl_2(*trans*)···MgH_2(**L**) complexes are 0.0105 a.u. and 0.0088 a.u., respectively. Evidently, the $\rho_{H\cdots H}$ in the **S** structure is larger than that in **L** structure. A similar result is also found between $C_2HCl_3\cdots MgH_2$(**S**) and $C_2HCl_3\cdots MgH_2$(**L**) complexes. For C_2-H_2Cl_2(*cis*)···MgH_2, $C_2H_2Cl_2$(*trans*)···MgH_2 and $C_2HCl_3\cdots MgH_2$ complexes, however, the differences in $\rho_{H\cdots H}$ between **F** structure and **L** structure are 0.0003, −0.0005, and −0.0007, respectively. In other words, the intensity of H···H interaction is enhanced within the **S** structure but negligible effect in **F** structure. Additionally, in **S** and **F** structures, the electron density ρ [0.010–0.014 a.u.] and Laplacian $\nabla^2\rho$ [0.048–0.066 a.u.] at the Mg···Cl BCPs also fall within the proposed range for weak interaction as well. It is pointed out that, the values of ρ and $\nabla^2\rho$ at the Mg···Cl BCPs decrease as the increase of substituent Cl atom numbers, which is consistent with the trend of interaction energies for **S** and **F** structures discussed above. Thus, it suggests that the Mg···Cl interactions in cyclic structures

Table 3 Electron densities ρ (a.u.) and Laplacians $\nabla^2\rho$ (a.u.) of the bond critical points (BCPs) in the $C_2H_{4-n}Cl_n\cdots MgH_2$ (n = 0, 1, 2, 3) complexes

Complex	ρ_{C-H}	$\Delta\rho_{C-H}$[a]	$\rho_{H\cdots H}$	$\nabla^2\rho_{H\cdots H}$	ρ_{H-Mg}	$\Delta\rho_{H-Mg}$[a]	$\rho_{Mg\cdots Cl}$	$\nabla^2\rho_{Mg\cdots Cl}$
L structure								
$C_2H_4\cdots MgH_2$	0.2875	0.0016	0.0047	0.0120	0.0525	−0.0002		
$C_2H_3Cl\cdots MgH_2$	0.2873	0.0015	0.0058	0.0142	0.0523	−0.0004		
$C_2H_2Cl_2$(*cis*)···MgH_2	0.2932	0.0015	0.0088	0.0214	0.0520	−0.0006		
$C_2H_2Cl_2$(*trans*)···MgH_2	0.2937	0.0012	0.0088	0.0216	0.0522	−0.0005		
$C_2HCl_3\cdots MgH_2$	0.2937	0.0007	0.0098	0.0241	0.0520	−0.0006		
S structure								
$C_2H_3Cl\cdots MgH_2$	0.2899	0.0030	0.0078	0.0195	0.0510	−0.0016	0.0122	0.0622
$C_2H_2Cl_2$(dic)···MgH_2	0.2897	0.0021	0.0088	0.0215	0.0513	−0.0013	0.0108	0.0525
$C_2H_2Cl_2$(*trans*)···MgH_2	0.3034	0.0109	0.0105 (0.0017[b])	0.0257	0.0539	0.0012	0.0121	0.0574
$C_2HCl_3\cdots MgH_2$	0.2940	0.0011	0.0111 (0.0013[b])	0.0266	0.0513	−0.0014	0.0101	0.0481
F structure								
$C_2H_3Cl\cdots MgH_2$	0.2944	0.0019	0.0083	0.0223	0.0505	−0.0021	0.0136	0.0700
$C_2H_2Cl_2$(*cis*)···MgH_2	0.3020	0.0103	0.0091 (0.0003[b])	0.0236	0.0534	0.0007	0.0138	0.0659
$C_2H_2Cl_2$(*trans*)···MgH_2	0.2936	0.0011	0.0083 (−0.0005[b])	0.0227	0.0508	−0.0018	0.0125	0.0623
$C_2HCl_3\cdots MgH_2$	0.2936	0.0006	0.0091 (−0.0007[b])	0.0246	0.0508	−0.0018	0.0122	0.0601

[a] The difference in the electron density between the complex and monomer. [b] Data in parentheses are the difference of electron densities between the ring structure (**S** or **F**) and **L** structure for the same complex.

account for a high proportion in the interaction energies. As shown in Table 2, **F** structures are more stable than **S** structures. It can be partially explained by the fact that for the complexes containing the same number of Cl-substituents, $\rho_{Mg\cdots Cl}$ value in **F** structure is greater than those in **S** structure (see Table 3).

3.3 NBO analysis

To reveal the nature of C(sp^2)–H⋯H DHB systems, we performed an analysis of natural bond orbital (NBO). Table 4 presents the charge transfer in the interaction and the NPA atom charge of direct participation in the dihydrogen bond. Generally, in dihydrogen bonds, the charge of the H atom in C–H proton donating bond is positive and the charge of the other H atom is negative. However, for all complexes, the H(–Mg) charge approximately amounts to −0.74 *e*. This is different from the H(–C) atom charges because of electronegativity of introduced Cl atoms. Analyzing the computational results, the charge on the H(–C) atom increases according as following trend for the donating molecules: C_2H_4 < C_2H_3Cl < $C_2H_2Cl_2$(*cis*, *trans* and dic) < C_2HCl_3. More atom charges in the dihydrogen bond mean that electrostatic force play a great role in this interaction.

Charge transfer from the proton acceptor to the proton donor is a defining characteristic of both conventional hydrogen bonds and dihydrogen bonds. From Table 4, the total charges are transferred from MgH_2 to $C_2H_{4-n}Cl_n$ in **L** structure, which accorded with the previous correlations found for DHB systems.[26,53] For **L** structure, the values of charge transfer in $C_2H_4\cdots MgH_2$(0.004), $C_2H_3Cl\cdots MgH_2$(0.006), $C_2H_2Cl_2$(*cis* and *trans*)⋯MgH_2(0.009 and 0.011), and $C_2HCl_3\cdots MgH_2$(0.013) have the trend of $C_2H_4\cdots MgH_2$ < $C_2H_3Cl\cdots MgH_2$ < $C_2H_2Cl_2$(*cis* and *trans*)⋯MgH_2 < $C_2HCl_3\cdots MgH_2$. The interaction energies (exactly the H⋯H binding energies for **L** structure) have same order in the **L** structure. On the contrary, the values of transferred net charges from $C_2H_{4-n}Cl_n$ to MgH_2 within **S** and **F** structures decreased along with the augment of substituent Cl atoms. We conclude that the present investigation substantiates our earlier study on $C_2H_{4-n}Cl_n\cdots NaH$ (n = 0, 1, 2, 3) system which indicated that the direction of CT is affected by the formation of cyclic structure.[31]

We then dissected the charge-transfer manifold using NBO analysis, pinpointing the pivotal donor–acceptor interactions that directly engage the C–H and H–Mg bonds within the dihydrogen contact. The stabilization energies $E^{(2)}$ for $C_2H_{4-n}Cl_n\cdots MgH_2$ (n = 0, 1, 2, 3) complexes calculated at MP2/6-311++G(d,p) level are presented in Table 5. The NBO parameters reveal that, for C(sp^2)–H⋯H–Mg DHBs, the contributions originated from the interaction of σ(Mg–H) → RY*(H) and σ(Mg–H) → σ*(C–H), but the lp(Cl) → σ*(Mg–H) overlap was responsible for the existence of Mg⋯Cl interaction. It is worth to notice that the $E^{(2)}$ values for $C_2H_3Cl\cdots MgH_2$(**F**) complex are corresponding to the lp(Cl) → σ(Mg–H) overlap. During the formation of the $C_2H_{4-n}Cl_n\cdots MgH_2$ (n = 0, 1, 2, 3) complexes, the advance of electronic density in the antibonding orbital of C–H bond leads to bond elongation and red shift of the respective stretching vibrational which is similar to conventional hydrogen bonds (except for $C_2H_3Cl\cdots MgH_2$(**F**) and $C_2H_2Cl_2$(*cis*)⋯MgH_2(**F**) complexes where σ*(C–H) are meaningless decrease upon complexation).[49,54] Similar observation can be obtained from Mg–H bond, and the occupation difference value of Δσ*(Mg–H) is greater than that of Δσ*(C–H) in specific complex. Especially, an unusual increase of the σ*(Mg–H) occupation for $C_2H_3Cl\cdots MgH_2$(**F**) complex is given by NBO analysis, value reached 1.8636, however, we cannot explain this in present study. Briefly, for the **S** and **F** structures the lp(Cl) → σ*(Mg–H) orbital interaction lead to an increase in the population of the antibonding Mg–H orbital, which in turn causes elongation of the Mg–H bond. Furthermore, as shown in Fig. 2, there is a roughly linear relationship (with a linear regression correlation coefficient R^2 = 0.77) between the occupation difference value of Δσ*(C–H) and its corresponding bond length variation (Δr), that is to say, the more Δσ*(C–H) is, the higher value of Δr(C–H) would be. Similar results are also found for proton accepting Mg–H bond.

The directions and the amounts of charge transfer along the C(sp^2)–H⋯H–Mg dihydrogen bond and H–Mg⋯Cl interactions within these complexes are illustrated in Fig. 3. Very roughly the 0.001 *e* of charge transfer corresponds to 1 kcal mol^{-1} of the stabilization energy.[1] Therefore, from Fig. 3, it is evident that the net charge is moved from MgH_2 to $C_2H_{4-n}Cl_n$ (n = 0, 1, 2, 3) in **L** structure. The analogous transitions in **S** and **F** structures are intricate. NBO analysis shows that the charge transfer in **S** and **F** structures is bidirectional. As shown in Fig. 3, more significant charge is transferred from the lone electron pairs of Cl atom to the antibonding σ*(Mg–H) orbital in the complex forming **S** and **F** structures. It reveals that more charge is transferred from $C_2H_{4-n}Cl_n$ (n = 1, 2, 3) to MgH_2 segment along the H–Mg⋯Cl bond than returned charge from MgH_2 to $C_2H_{4-n}Cl_n$ (n = 1, 2, 3) through the C–H⋯H–Mg dihydrogen

Table 4 Charge transfer (CT, *e*), NPA atom charges (*q*, *e*) and charge change of H atoms (Δ*q*, *e*) in the $C_2H_{4-n}Cl_n\cdots MgH_2$ (n = 0, 1, 2, 3) complexes

Complex	$q_{H(C)}$	$\Delta q_{H(C)}$	$q_{H(Mg)}$	$\Delta q_{H(Mg)}$	CT
L structure					
$C_2H_4\cdots MgH_2$	0.184	0.013	−0.720	−0.009	0.004[a]
$C_2H_3Cl\cdots MgH_2$	0.206	0.014	−0.728	−0.017	0.006[a]
$C_2H_2Cl_2$(*cis*)⋯MgH_2	0.228	0.021	−0.738	−0.027	0.009[a]
$C_2H_2Cl_2$(*trans*)⋯MgH_2	0.225	0.018	−0.737	−0.025	0.011[a]
$C_2HCl_3\cdots MgH_2$	0.240	0.020	−0.740	−0.029	0.013[a]
S structure					
$C_2H_3Cl\cdots MgH_2$	0.222	0.030	−0.740	−0.029	0.024[b]
$C_2H_2Cl_2$(dic)⋯MgH_2	0.236	0.031	−0.737	−0.026	0.018[b]
$C_2H_2Cl_2$(*trans*)⋯MgH_2	0.244	0.037	−0.741	−0.030	0.018[b]
$C_2HCl_3\cdots MgH_2$	0.257	0.037	−0.738	−0.026	0.012[b]
F structure					
$C_2H_3Cl\cdots MgH_2$	0.227	0.037	−0.746	−0.035	0.027[b]
$C_2H_2Cl_2$(*cis*)⋯MgH_2	0.246	0.038	−0.746	−0.035	0.024[b]
$C_2H_2Cl_2$(*trans*)⋯MgH_2	0.243	0.036	−0.743	−0.032	0.023[b]
$C_2HCl_3\cdots MgH_2$	0.257	0.038	−0.743	−0.032	0.022[b]

[a] Charge transfer from MgH_2 to $C_2H_{4-n}Cl_n$. [b] Charge transfer from $C_2H_{4-n}Cl_n$ to MgH_2.

Table 5 The selected second-order perturbation energies, $E^{(2)}$ (kcal mol^{-1}), and the electron occupation differences at the C–H and Mg–H antibonding orbitals from an NBO analysis[a] of the $C_2H_{4-n}Cl_n\cdots MgH_2$ (n = 0, 1, 2, 3) complexes at the MP2/6-311++G(d,p) level

Complex	$E^{(2)}$ lp(Cl) → σ*(Mg–H)			$E^{(2)}$ σ(Mg–H) → RY*H		σ(Mg–H) → σ*(C–H)	Δσ*(C–H)[b]	Δσ*(Mg–H)[b]
Lstructure								
$C_2H_4\cdots MgH_2$				3.95	0.63	1.38	0.0001	0.0029
$C_2H_3Cl\cdots MgH_2$				6.19	0.74	2.23	0.0006	0.0055
$C_2H_2Cl_2$(*cis*)$\cdots MgH_2$				7.91	1.31	4.82	0.0016	0.0077
$C_2H_2Cl_2$(*trans*)$\cdots MgH_2$				8.16		4.51	0.0027	0.0082
$C_2HCl_3\cdots MgH_2$				9.18		5.44	0.0034	0.0096
Sstructure								
$C_2H_3Cl\cdots MgH_2$	2.17	3.29	4.68	0.51		1.64	0.0018	0.0101
$C_2H_2Cl_2$(dic)$\cdots MgH_2$	1.85	1.36	5.42	0.70		2.52	0.0035	0.0092
$C_2H_2Cl_2$(*trans*)$\cdots MgH_2$	2.24	6.71		0.64		3.71	0.0040	0.0101
$C_2HCl_3\cdots MgH_2$	1.94		5.45	0.67		4.64	0.0059	0.0094
Fstructure								
$C_2H_3Cl\cdots MgH_2$	1.83[c]		7.88[c]			1.28	−0.0008	1.8636
$C_2H_2Cl_2$(*cis*)$\cdots MgH_2$	1.95	7.26				1.61	−0.0003	0.0121
$C_2H_2Cl_2$(*trans*)$\cdots MgH_2$	1.92	1.28	5.91			1.62	0.0005	0.0113
$C_2HCl_3\cdots MgH_2$	1.97	6.64		0.57		2.06	0.0011	0.0116

[a] σ* denotes the formally empty antibonding orbital, lp denotes the occupied lone pair. [b] The electron occupation difference between the C–H (Mg–H) antibonding orbital in the complex and the isolated proton donor (acceptor). [c] The value of the stabilization energy is due to the lp(Cl) → σ(Mg–H) orbital interaction.

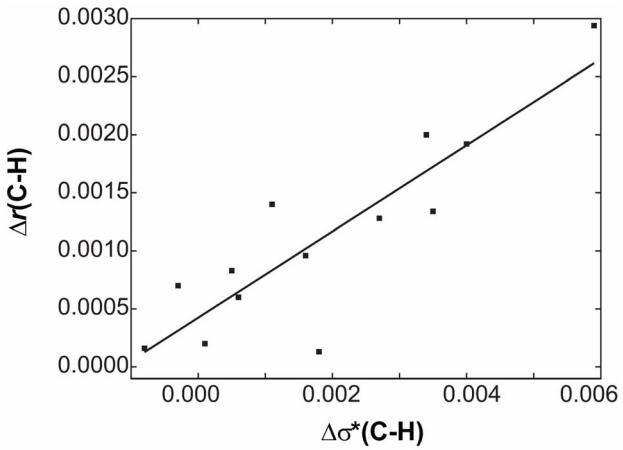

Fig. 2 Correlation between the elongation of the C–H proton-donating bond (in Å) and the increase in electron density within the σ*(C–H) orbital (in *e*).

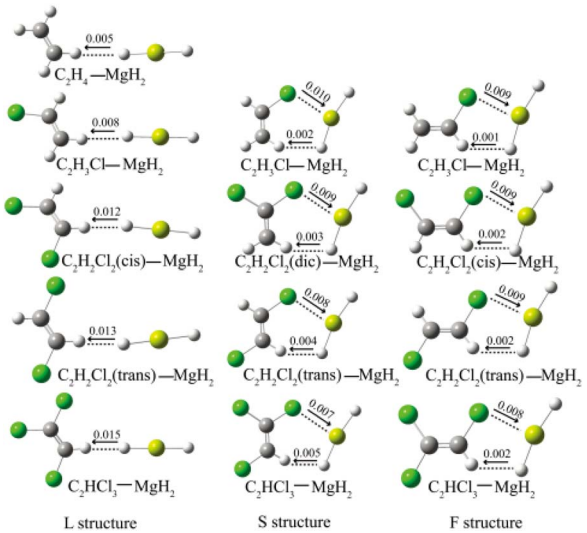

Fig. 3 The directions and the amount of the charge transfer along the C(sp^2)–H···H–Mg dihydrogen bond and H–Mg···Cl interaction.

bond (see Fig. 3). As a consequence, the final transfer net charge is from the proton donor $C_2H_{4-n}Cl_n$ (n = 1, 2, 3) to the proton acceptor MgH_2 within the **S** and **F** type complexes, which is contrary to the previous found for traditional hydrogen bonds and DHB systems. With increasing the number of chlorine atoms in ethylene, the amount of charge transfer along C–H···H–Mg dihydrogen bond gains, while the value of charge flowing along H–Mg···Cl bond falls. Thus, the total transfer net charge in **S** and **F** structures decreases as following order, $C_2H_3Cl\cdots MgH_2$ > $C_2H_2Cl_2$ (*cis*, *trans* and dic types)$\cdots MgH_2$ > $C_2HCl_3\cdots MgH_2$.

4. Conclusions

In this article, we systematically investigated the characteristics of dihydrogen bonds between MgH_2 and ethylene, as well as its chlorine derivatives, at the MP2/6-311++G(d,p) level of theory. The systems studied here were finally classified into three types based on the optimized structures. Geometrical, energetic, and topological parameter analyses indicate that the $C_2H_4\cdots MgH_2$ and $C_2H_3Cl\cdots MgH_2$(**L**) complexes should be categorized as van

der Waals complexes. The remaining complexes involve dihydrogen bond interactions with conventional hydrogen-bond strength. For most complexes, complexation induced a lengthening of the proton-donating C–H bond, accompanied by a corresponding red shift in the stretching frequency. Calculation results suggest that the strength of the H···H interaction increases with the introduction of more chlorine atoms on the ethylene skeleton. Concurrently, charge transfer from MgH_2 to $C_2H_{4-n}Cl_n$ ($n = 0, 1, 2, 3$) *via* the C–H···H–Mg dihydrogen bonds increases in the same order. AIM analysis reveals the electrostatic nature of the C(sp^2)–H···H interaction in all dihydrogen-bonded complexes.

Dihydrogen bonds and Mg···Cl interactions coexist in both the **S** and **F** structures. The impact of the formed ring structures on the H···H bond in $C_2H_{4-n}Cl_n\cdots MgH_2$ ($n = 0, 1, 2, 3$) complexes was investigated. Compared with the **L** structure (containing only H···H interactions), the formation of Mg···Cl bonds significantly increases the H···H bond length and reverses the direction of charge transfer, contrasting with previous findings. Additionally, the H···H interaction strength is enhanced in the **S** structure but exhibits negligible changes in the **F** structure. In the **S** type conformer, an optimal charge distribution and structural arrangement synergistically strengthen the H···H interaction, whereas the **F** conformer is strained and its H···H contact is attenuated by competing Mg···Cl interactions—trends fully mirrored in the AIM metrics and interaction energies. Thus, structural flexibility is decisive: the six-membered ring can subtly relax to accommodate the dihydrogen bond, and the embedded C(sp^2)=C(sp^2) π-system further facilitates charge delocalization. Together, these synergistic effects produce a cooperative enhancement that markedly stabilizes the entire interaction network.

Author contributions

Conceptualization, Fu-Quan Bai, Xiang Guo and Xianping Qiu; data curation, Lu Feng, Xianping Qiu, Yin-Si Ma, Zhixiong Tian and Kehai Chen; funding acquisition, Fu-Quan Bai and Xiang Guo; validation, Lu Feng and Si Zhang; writing – original draft, Lu Feng and Fu-Quan Bai; writing – review & editing, Xiang Guo, Xianping Qiu and Fu-Quan Bai.

Conflicts of interest

There are no conflicts to declare.

Data availability

The data supporting the findings of this article are included in the manuscript and are available upon reasonable request from the corresponding author.

Acknowledgements

This work was funded by the Open Research Fund Program of National Key Laboratory of Aerospace Chemical Power (STACPL120221B02) and the LIXIN Outstanding Young Scholar Training Program of Jilin University.

Notes and references

1 R. P. Bu, Y. Xiong, X. F. Wei, H. Z. Li and C. Y. Zhang, *Cryst. Growth Des.*, 2019, **19**(10), 5981–5997.
2 Q. Li, T. Hu, X. An, W. Li, J. Cheng, B. Gong and J. Sun, *ChemPhysChem*, 2009, **10**, 3310–3315.
3 G. R. Liu, S. H. Wei and C. Y. Zhang, *Cryst. Growth Des.*, 2020, **20**(10), 7065–7079.
4 Y. X. Wang, K. L. Dou, J. L. Liu, L. Zhang, L. Hu and S. P. Pang, *Chem.–Eur. J.*, 2025, **31**(28), e202500884, DOI: **10.1002/chem.202500884**.
5 W. Qin, X. Guo, J. Xiao, Z. Guan, X. Qiu and F. Q. Bai, *Int. J. Hydrogen Energy*, 2024, **110**, 430–444.
6 L. Feng, F. Q. Bai, Y. Wu and H. X. Zhang, *Sci. China: Chem.*, 2012, **55**(2), 262–269.
7 X. Yang and M. B. Hall, *J. Am. Chem. Soc.*, 2009, **131**, 10901–10908.
8 L. J. Karas, C. H. Wu, R. Das and J. I. C. Wu, *Wiley Interdiscip. Rev.: Comput. Mol. Sci.*, 2020, **10**(6), e1477.
9 C. J. Cramer and W. L. Gladfelter, *Inorg. Chem.*, 1997, **36**, 5358–5362.
10 P. E. M. Siegbahn, O. Eisenstein, A. L. Rheingold and T. F. Koetzle, *Acc. Chem. Res.*, 1996, **29**, 348–354.
11 T. B. Richardson, T. F. Koetzle and R. H. Crabtree, *Inorg. Chim. Acta*, 1996, **250**, 69–73.
12 Q. Liu and R. Hoffmann, *J. Am. Chem. Soc.*, 1995, **117**, 10108–10112.
13 S. A. Kulkarni, *J. Phys. Chem. A*, 1999, **103**, 9330–9335.
14 B. G. Oliveira, R. C. M. U. Araújo and M. N. Ramos, *Struct. Chem.*, 2008, **19**(4), 665–670.
15 H. Y. Wang, Y. L. Zeng, S. J. Zheng and L. P. Meng, *Acta Phys.-Chim. Sin.*, 2007, **23**(7), 1131–1135.
16 R. Custelcean and J. E. Jackson, *Chem. Rev.*, 2001, **101**, 1963–1980.
17 Q. Li, Y. F. Xie, Z. P. Wang, S. Li, S. Y. Yang, D. Z. Yang, L. Zhang, G. H. Du and Y. Lu, *RSC Adv.*, 2024, **14**(54), 40006–40017.
18 K. T. Mahmudov, M. N. Kopylovich, M. F. C. G. da Silva and A. J. L. Pombeiro, *Coord. Chem. Rev.*, 2017, **345**, 54–72.
19 T. Richardson, S. de Gala, R. H. Crabtree and P. E. M. Siegbahn, *J. Am. Chem. Soc.*, 1995, **117**, 12875–12876.
20 I. I. Padilla-Martińez, M. D. J. Rosalez-Hoz, H. Tlahuext, C. Camacho-Camacho, A. Ariza-Castolo and R. Contreras, *Chem. Ber.*, 1996, **129**, 441–449.
21 S. A. Kulkarni and A. K. Srivastava, *J. Phys. Chem. A*, 1999, **103**, 2836–2842.
22 R. Custelcean and J. E. Jackson, *Chem. Rev.*, 2001, **101**, 1963–1980.
23 D. Yu, D. Wu, J. Y. Liu, S. Y. Li and Y. Li, *RSC Adv.*, 2020, **10**(57), 34413–34420.
24 S. J. Grabowski, W. A. Sokalski and J. Leszczynski, *J. Phys. Chem. A*, 2005, **109**, 4331–4341.
25 W. Zierkiewicz and P. Hobza, *Phys. Chem. Chem. Phys.*, 2004, **6**, 5288–5296.

26 Y. Wu, L. Feng and X. D. Zhang, *J. Mol. Struct.: THEOCHEM*, 2008, **851**, 294–298.
27 P. Lipkowski, S. J. Grabowski, T. L. Robinson and J. Leszczynski, *J. Phys. Chem. A*, 2004, **108**, 10865–10872.
28 H. Cybulski, E. Tyminska and J. Sadlej, *ChemPhysChem*, 2006, **7**, 629–639.
29 K. N. Robertson, O. Knop and T. S. Cameron, *Can. J. Chem.*, 2003, **81**, 727–743.
30 H. Cybulski, M. Pecul, J. Sadlej and T. Helgaker, *J. Chem. Phys.*, 2003, **119**, 5094–5104.
31 L. Feng, F. Q. Bai, Y. Wu and H. Zhang, *Mol. Phys.*, 2011, **109**(5), 645–653.
32 P. C. Singh and G. N. Patwari, *Chem. Phys. Lett.*, 2006, **419**(1–3), 5–9.
33 Y. G. Yang, Y. F. Liu, D. P. Yang, H. Li, K. Jiang and J. F. Sun, *Phys. Chem. Chem. Phys.*, 2015, **17**(48), 32132–32139.
34 P. D. Duraisamy, P. Gopalan and A. Angamuthu, *Monatsh. Chem.*, 2020, **151**, 1569–1579.
35 B. Bogdanović, *Angew. Chem., Int. Ed. Engl.*, 1985, **24**, 262–273.
36 R. F. W. Bader, *Atoms in Molecules: a Quantum Theory*, Clarendon Press, Oxford, New York, 1990.
37 M. J. Frisch, G. W. Trucks, H. B. Schlegel and G. E. Scuseria, *et al.*, *Gaussian 16*, Gaussian, Inc., Wallingford, CT, 2016.
38 A. Shayesteh, D. R. T. Appadoo, I. Gordon and P. F. Bernath, *J. Chem. Phys.*, 2003, **119**, 7785–7788.
39 F. Sim, A. St. Amant, I. Papai and D. R. Salahub, *J. Am. Chem. Soc.*, 1992, **114**, 4391–4400.
40 A. D. Boese, A. Chandra, J. M. L. Martin and D. Marx, *J. Chem. Phys.*, 2003, **119**, 5965–5980.
41 M. Alkorta, J. Elguero and S. J. Grabowski, *J. Phys. Chem. A*, 2008, **112**, 2721–2727.
42 S. J. Grabowski, *J. Mol. Struct.*, 2000, **553**, 151–156.
43 B. Chan and J. Ho, *J. Phys. Chem. A*, 2023, **127**(47), 10026–10031.
44 S. F. Boys and F. Bernardi, *Mol. Phys.*, 1970, **19**, 553–566.
45 *AIM2000 Designed by Friedrich Biegler-König*, University of Applied Sciences, Bielefeld, Germany, 2002.
46 A. E. Reed, L. A. Curtiss and F. Weinhold, *Chem. Rev.*, 1988, **88**, 899–926.
47 S. J. Grabowski, *J. Phys. Chem. A*, 2000, **104**, 5551–5557.
48 S. J. Grabowski, T. L. Robinson and J. Leszczynski, *Chem. Phys. Lett.*, 2004, **386**, 44–48.
49 D. Parimala devi, G. Praveena, R. Jeba Beula, *et al.*, *J. Struct. Chem.*, 2022, **63**, 501–509.
50 P. devi Duraisamy, S. Prince Makarios Paul, P. Gopalan, *et al.*, *Russ. J. Phys. Chem. A*, 2023, **97**, 3068–3080.
51 I. Alkorta, K. Zborowski, J. Elguero and M. Solimannejad, *J. Phys. Chem. A*, 2006, **110**, 10279–10286.
52 P. L. A. Popelier, *J. Phys. Chem. A*, 1998, **102**, 1873–1878.
53 S. J. Grabowski, W. A. Sokalski and J. Leszczynski, *J. Phys. Chem. A*, 2005, **109**, 4331–4341.
54 J. Chocholousova, V. Spirko and P. Hobza, *Phys. Chem. Chem. Phys.*, 2004, **6**, 37–41.